Monatshefte für Chemie 129, 649–660 (1998)

Monatshefte für Chemie
Chemical Monthly

Printed in Austria

Induction of Wavelength-Dependent Photochemistry in Bilirubins by Serum Albumin

Antony F. McDonagh[1,*], **Giovanni Agati**[2], and **David A. Lightner**[3]

[1] Division of Gastroenterology, Box 0538, S-357, University of California, San Francisco, CA 94143-0538, USA
[2] Istituto di Elettronica Quantistica, CNR, Sezione INFM di Firenze, I-50127 Firenze, Italy
[3] Department of Chemistry, University of Nevada, Reno, NV 89557-0020, USA

Summary. Quantum yields for $Z \rightleftarrows E$ photoisomerization of the natural bi-chromophore bilirubin IXα in ammoniacal methanol solution were found to vary with excitation wavelength, whereas no variation (within experimental error) was observed for xanthobilirubic acid and for symmetrically substituted bilirubins (bilirubin IIIα, bilirubin XIIIα, and mesobilirubin XIIIα) in the same solvent. The quantum yield for $Z \rightleftarrows E$ photoisomerization of xanthobilirubic acid bound to human serum albumin was also invariant with excitation wavelength. In contrast, quantum yields for $Z \rightleftarrows E$ photoisomerization of the symmetrically-substituted bilirubins did show marked excitation wavelength dependency when they were bound to human serum albumin. These results show that quantum yields for $Z \rightleftarrows E$ photoisomerization of bilirubins are markedly sensitive to protein binding and to the nature of pyrrole ring β-substituents. They also demonstrate that wavelength-dependent photochemistry is characteristic of bilirubins with non-identical pyrromethenone chromophores, as expected from exciton coupling theory, and that complexation with albumin induces wavelength-dependent photochemistry in symmetrically substituted bilirubins.

Keywords. Bile pigments; Exciton coupling; Human serum albumin; Phototherapy; Pyrromethenone.

Induktion einer wellenlängenabhängigen Photochemie in Bilirubin durch Serumalbumin

Zusammenfassung. Die Quantenausbeuten der $Z \rightleftarrows E$ Photoisomerisierung des natürlichen bichromophoren Bilirubins IXα in ammoniakalisch-methanolischer Lösung variieren mit der Anregungswellenlänge, wogegen (innerhalb des experimentellen Fehlers) für Xanthobilirubinsäure und symmetrisch substituierte Bilirubine (Bilirubin IIIα, und XIIIα, sowie Mesobilirubin XIIIα) im selben Lösungsmittel keine solche Variation zu beobachten war. Die Quantenausbeute der $Z \rightleftarrows E$ Photoisomerisierung von Xanthobilirubinsäure, die an Serumalbumin gebunden ist Wurde ebenfalls als invariant in Bezug auf die Anregungswellenlänge gefunden. Demgegenüber zeigten die Quantenausbeuten der $Z \rightleftarrows E$ Photoisomerisierung symmetrisch substituierter Bilirubine eine ausgeprägte Abhängigkeit von der Wellenlänge, wenn sie an Serumalbumin gebunden waren. Diese Ergebnisse zeigen, daß die Quantenausbeuten der $Z \rightleftarrows E$ Photoisomerisierung von Bilirubinen sehr

* Corresponding author

empfindlich in Hinblick auf Proteinbindung und die Natur der Pyrrol-β-Substituenten sind. Sie demonstrieren weiters daß die wellenlängenabhängige Photochemie charakteristisch für Bilirubine mit nicht-identischen Dipyrrin-chromophoren ist, wie dies aus der Excitonkopplungstheorie erwartet werden kann, und daß die Komplexierung mit Albumin auch eine wellenlängenabhängige Photochemie in symmetrisch substituierten Bilirubinen induziert.

Introduction

Quantum yields for photochemical reactions do not generally vary with excitation wavelength [1]. But exceptions to this generalization are not uncommon – one being the $Z \rightleftarrows E$ photoisomerization of bilirubin (*BR*) (**1**, Fig. 1) in solutions containing equimolar or greater concentrations of human serum albumin (HSA) [2]. Bilirubin is a bichromophoric molecule, biosynthesized from heme, that circulates in blood as a reversible association complex with albumin. Its complex with human serum albumin ($BR \cdot$ HSA) has a broad absorption band peaking at about 460 nm and extending to about 530 nm. When people are exposed to light with wavelengths in this region, bilirubin in blood and other tissues undergoes reversible photoisomerization from the biosynthetic 4*Z*,15*Z* form (**1**) to the isomeric 4*Z*,15*E* (**2**) and 4*E*,15*Z* (**3**) forms [3, 4]. Because these three diastereomers have extensively overlapping absorption bands, a photoequilibrium mixture of all of them (along with a small amount of the 4*E*,15*E* isomer) is eventually formed when $BR \cdot$ HSA solutions are irradiated *in vitro* [5]. Complexation of bilirubin with proteins has a strong influence on the regioselectivity of its photochemistry. In the case of the $BR \cdot$ HSA complex, the proportion of 4*E*,15*Z* and 4*E*,15*E* isomers that is present at photoequilibrium is very small compared to the proportion of the 4*Z*,15*E* isomer [3, 6]. Photoisomerization of bilirubin in humans has no known physiological function, but the reaction is important in phototherapy of newborn babies with severe jaundice and in the treatment of patients with the rare hereditary *Crigler-Najjar* syndrome [7, 8].

The quantum yield ($\Phi_{Z,Z\rightarrow Z,E}$) for $Z \rightarrow E$ photoisomerization of $BR \cdot$ HSA *in vitro* varies with excitation wavelength, decreasing from 0.1 to 0.05 with increasing

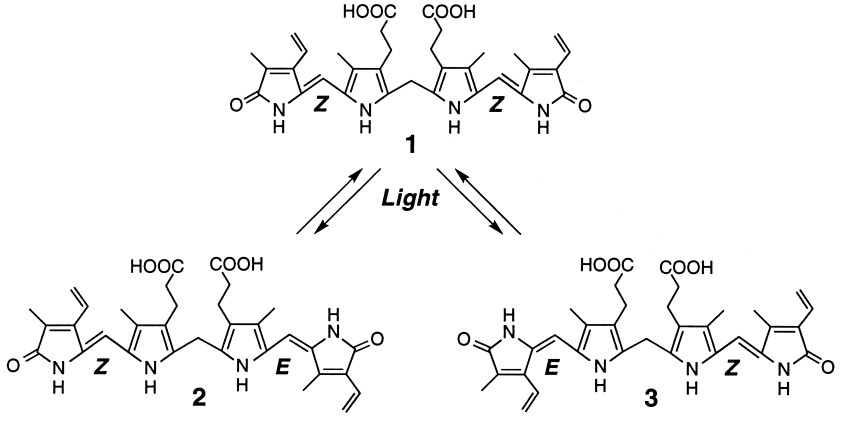

Fig. 1. Linear representations of 4*Z*,15*Z*-bilirubin IXα (**1**) and its 4*Z*,15*E* (**2**) and 4*E*,15*Z* (**3**) configurational isomers

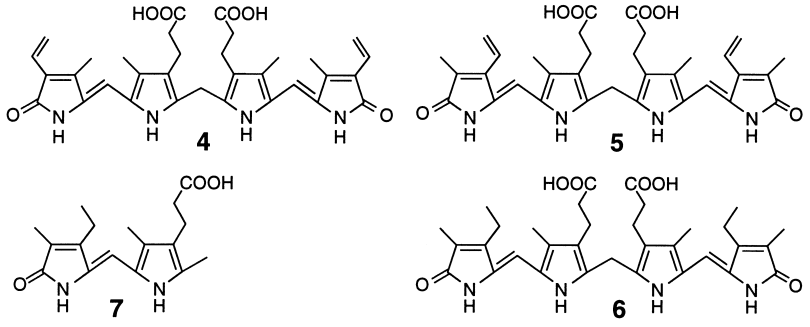

Fig. 2. Chemical structures of 4*Z*,15*Z*-bilirubin IIIα (**4**), 4*Z*,15*Z*-bilirubin XIIIα (**5**), 4*Z*,15*Z*-mesobilirubin XIIIα (**6**), and *Z*-xanthobilirubic acid (**7**)

excitation wavelength over the range 457.9–514.5 nm [2]. This phenomenon has been attributed to exciton coupling [9] and intramolecular partitioning of excitation energy between the two similar, but non-identical, dipyrrinone chromophores of the protein-linked pigment [2, 10–12]. The exciton model, which is based on a more rigorous quantum mechanical treatment, also predicts wavelength-dependent photochemistry for *BR* even when it is not bound to protein. However, that prediction has not been demonstrated experimentally, and it is unclear whether the observed variation of quantum yield with excitation wavelength for photoisomerization of *BR* · HSA in aqueous solutions is an inherent property of the chromophore or is engendered solely by its association with protein. To distinguish these contributions, we have measured quantum yields for the photoisomerization of *BR* and several closely related model compounds (Fig. 2, **4–7**) in protein-free methanolic solutions and in aqueous solutions containing excess HSA. Our results are consistent with the exciton coupling explanation for the wavelength-dependent photochemistry of bilirubin. They show that wavelength-dependent photochemistry is an inherent property of the pigment which is augmented by binding to albumin. For symmetrically substituted bilirubins, such as **4, 5** and **6**, quantum yields for photoisomerization are independent of excitation wavelength in the absence of protein, but wavelength dependent in its presence. Protein binding, therefore, can effectively ''de-symmetrize'' symmetrical bichromophoric molecules and induce wavelength-dependent photochemistry.

Results

For all compounds studied, *E* photoisomers were readily separated from the less polar parent *Z* isomers by HPLC. Formation of photooxidation products and of isomers other than *Z*,*E* was negligible under the experimental conditions used.

Xanthobilirubic acid

Quantum yields for $Z \rightarrow E$ photoisomerization of xanthobilirubic acid (*XBR*, **7**) at different excitation wavelengths are given in Table 1. In both methanolic and HSA solutions, values of $\Phi_{Z \rightarrow E}$ were substantial (0.19 and 0.12, respectively) and

Table 1. Quantum yields ($\Phi_{Z\rightarrow E}$) for $Z\rightarrow E$ photoisomerization of xanthobilirubic acid (**7**) in 0.1% NH_4OH/MeOH and HSA solutions

Excitation wavelength (nm)	$\Phi_{Z\rightarrow E}$	
	NH_4OH/MeOH[a]	HSA[a]
390	0.197 ± 0.010	
410	0.190 ± 0.006	
430	0.192 ± 0.010	0.127 ± 0.003
440	0.184 ± 0.006	
460	0.182 ± 0.002	0.122 ± 0.005
470		0.122 ± 0.005

[a] Mean $\pm$ standard deviation

constant within the experimental error over the range of excitation wavelengths investigated. The value for *XBR* · HSA is much smaller than that reported previously (0.4; [13]). However, as noted elsewhere [2], the earlier value was based on an estimated $\Phi_{Z,Z\rightarrow Z,E}$ value of 0.2 for *BR* · HSA which has subsequently been shown to be incorrect.

Symmetric bilirubins

Quantum yields for $Z\rightarrow E$ photoisomerization of bilirubin IIIα (*BR*-III, **4**), bilirubin XIIIα (*BR*-XIII, **5**), and mesobilirubin XIIIα (*MBR*-XIII, **6**) are listed in Table 2. For all three compounds, $\Phi_{Z\rightarrow E}$ was significantly ($P > 0.1$) independent of excitation wavelength in NH_4OH/MeOH, with average values of 0.058, 0.013 and 0.041, respectively. When the pigments were complexed with HSA, however, $\Phi_{Z\rightarrow E}$ decreased significantly with increasing excitation wavelength ($P < 0.0005$), the greatest effect being observed with *BR*-III (Fig. 3). The maximum $\Phi_{Z\rightarrow E}$ values for *BR*-III and *MBR*-XIII in HSA solutions were only slightly different from those in NH_4OH/MeOH. In contrast, $\Phi_{Z\rightarrow E}$ at 460 nm for *BR*-XIII was four times greater in HSA solution than in NH_4OH/MeOH.

Bilirubin-IXα

Irradiation of *BR* (4*Z*,15*Z*) in NH_4OH/MeOH generated the corresponding 4*E*,15*Z* and 4*Z*,15*E* stereoisomers **2** and **3**. Quantum yields for their formation are given in Table 3 and plotted in Fig. 4 as a function of excitation wavelength. The quantum yield $\Phi_{Z,Z\rightarrow E,Z}$ for formation of the 4*E*,15*Z* isomer **3** is about one third of the quantum yield $\Phi_{Z,Z\rightarrow Z,E}$ for formation of the 4*Z*,15*E* stereoisomer **2** for excitation in the 430–470 nm range, but only about one half at 500 nm because of a decrease in $\Phi_{Z,Z\rightarrow Z,E}$ and an increase in $\Phi_{Z,Z\rightarrow E,Z}$. Our measured quantum yields are similar to those reported for the photoisomerization of bilirubin in chloroform/triethylamine solution at a single excitation wavelength (436 nm) [14]. $\Phi_{Z,Z\rightarrow Z,E}$ showed a weak but significant wavelength dependence, decreasing with increasing excitation wavelength. The effect was not so marked as for *BR* · HSA (reported

Table 2. Quantum yields ($\Phi_{Z\rightarrow E}$)[a] for $Z\rightarrow E$ photoisomerization of *BR*-III, *BR*-XIII and *MBR*-XIII in 0.1% NH_4OH/MeOH and HSA solutions

Excitation wavelength (nm)	*BR*-III (**4**)		*BR*-XIII (**5**)		*MBR*-XIII (**6**)	
	NH_4OH/MeOH	HSA	NH_4OH/MeOH	HSA	NH_4OH/MeOH	HSA
430					0.038 ± 0.001	0.035 ± 0.001
436			0.0143 ± 0.0008			
457.9	0.060 ± 0.002	0.078 ± 0.007	0.0130 ± 0.0003		0.039 ± 0.004	
460				0.054 ± 0.003		0.033 ± 0.002
470						0.027 ± 0.002
476.5	0.056 ± 0.006	0.077 ± 0.004			0.045 ± 0.005	
480						0.024 ± 0.002
488	0.058 ± 0.002	0.064 ± 0.004	0.0139 ± 0.0012			
490				0.043 ± 0.001		
501.7	0.058 ± 0.002	0.049 ± 0.005				
514.5	0.060 ± 0.004	0.034 ± 0.003	0.0130 ± 0.0008			
515				0.031 ± 0.002		

[a] Mean $\pm$ standard deviation

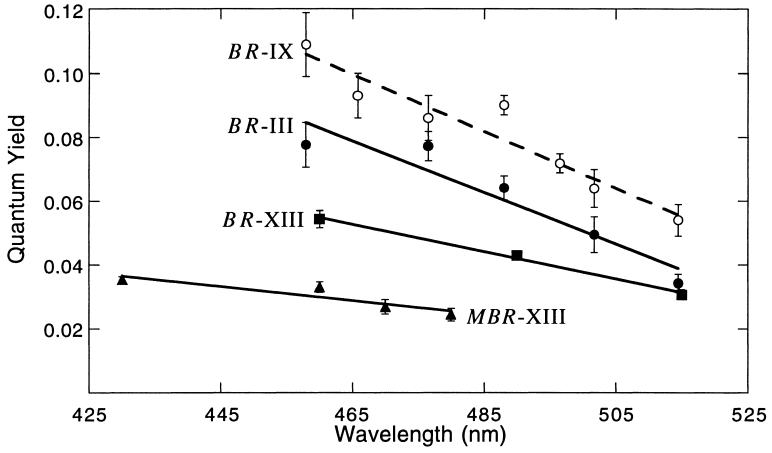

Fig. 3. Variation in quantum yield with excitation wavelength for $Z \rightarrow E$ photoisomerization of HSA complexes of 4*Z*,15*Z*-mesobilirubin XIIIα (**6**), 4*Z*,15*Z*-bilirubin XIIIα (**5**), and 4*Z*,15*Z*-bilirubin IIIα (**4**). The dashed curve shows previously published [2] quantum yields for the photoisomerization of 4*Z*,15*Z*-bilirubin IXα to 4*Z*,15*E*-bilirubin IXα under similar conditions

Table 3. Quantum yields for photoisomerization of 4*Z*,15*Z*-*BR*-IX (**1**) to 4*E*,15*Z*-*BR*-IX (**3**) ($\Phi_{Z,Z\rightarrow E,Z}$) and to 4*Z*,15*E*-*BR*-IX (**2**) ($\Phi_{Z,Z\rightarrow Z,E}$) in 0.1% NH_4OH/MeOH

Excitation wavelength (nm)	$\Phi_{Z,Z\rightarrow E,Z}$[a]	$\Phi_{Z,Z\rightarrow Z,E}$[a]
430	0.0080 ± 0.0002	0.0253 ± 0.0012
450	0.0085 ± 0.0005	0.0266 ± 0.0010
470	0.0082 ± 0.0006	0.0238 ± 0.0016
480	0.0086 ± 0.0007	0.0220 ± 0.0010
500	0.0103 ± 0.0004	0.0197 ± 0.0011

[a] Mean $\pm$ standard deviation

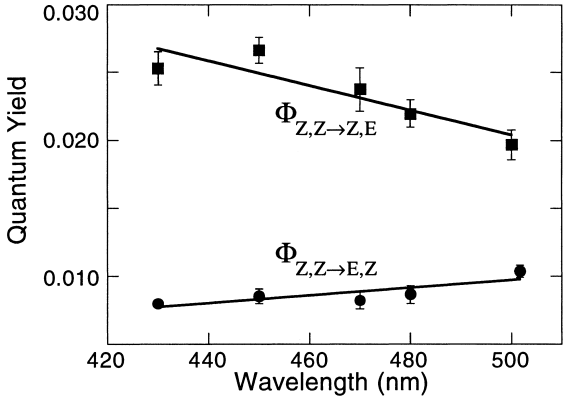

Fig. 4. Variation in quantum yields with excitation wavelength for the photoisomerization of 4*Z*,15*Z*-bilirubin IXα (**1**) to 4*Z*,15*E*-bilirubin IXα (**2**) and 4*E*,15*Z*-bilirubin IXα (**3**) in 0.1% NH_4OH/MeOH

previously [2] and shown in Fig. 3 (dashed curve) for comparison). $\Phi_{Z,Z\rightarrow E,Z}$ was constant within the experimental error between 430 and 480 nm, but increased by 24% at 500 nm.

Discussion

There is extensive spectroscopic and computational evidence that the methylene-linked dipyrrinone chromophores in excited-state bilirubins interact by electric dipole-dipole coupling, forming a molecular exciton [15–18]. Because of this, the first excited singlet state splits into two energy levels [9, 15, 19] and may be represented simplistically as a double minimum potential well (Fig. 5) from which decay, *via* twisted intermediates, can lead to ground-state photoisomers or starting material [10–12]. Decay to ground-state photoisomer from one well would correspond to isomerization in one of the rubin chromophores, decay from the other well to isomerization in the other chromophore. Competing with these decay pathways, but not depicted in the diagram, are radiationless internal conversions back to the ground state [20–23]. Luminescent pathways can be ignored because the quantum yield for fluorescence for bilirubin is very small [24].

For symmetrically substituted bilirubins, such as *BR*-III (**4**), *BR*-XIII (**5**) and *MBR*-XIII (**6**), the same *E*-isomer would be obtained, *via* identical twisted-state intermediates, from either of the two exciton states. Therefore, wavelength-dependent photochemistry would only be expected if the rate of radiationless decay from each exciton state to the common ground state were significantly different, which is unlikely. Consistent with this expectation, we were unable to detect significant variations in photoisomerization quantum yields with excitation wavelength for the three symmetrically substituted bilirubins in NH_4OH/MeOH.

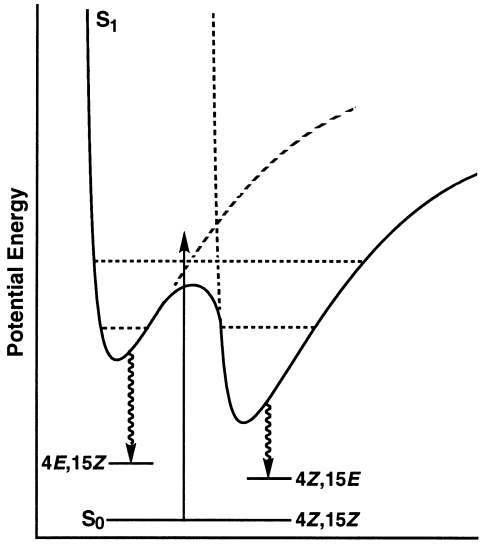

Fig. 5. Double-minimum potential energy model for the first excited singlet state of 4*Z*,15*Z*-bilirubin IX (**1**); horizontal dashed lines indicate excited vibronic levels

Similarly, unsymmetrically substituted bilirubins also have intrinsically two exciton states with potential energy wells of unequal depths. But, in this case, the two excitons can decay to non-identical diastereomeric ground states (and starting material), and their rates of decay might be different. For bilirubin IXα (**1**), the excitation energy may become localized either in the dipyrrinone with an *exo*-vinyl group or in the dipyrrinone with an *endo*-vinyl group. Decay from these states would then generate the respective diastereomeric 4*Z*,15*E* and 4*E*,15*Z* ground states or starting material. Thus, for both symmetrically and unsymmetrically substituted bilirubins the specific singlet (exciton) well into which the excitation energy eventually becomes localized, following decay from upper vibrational levels, may depend on the wavelength (energy) of excitation, but wavelength-dependent quantum yields for photoisomerization would be expected only for unsymmetrically substituted pigments in an achiral isotropic medium. Excitation of these pigments using energies that are large enough to populate singlet vibrational levels lying above the barrier between the wells would allow excitation to hop between the wells before eventually becoming trapped in one of them [25, 26]. Therefore, with short-wavelength excitation, quantum yields for isomerization would be expected to be independent of wavelength and dependent only on the relative depths of the wells and the relative rates of radiationless deactivation processes. But towards longer excitation wavelengths, the probability of excitation to vibronic levels higher than the barrier between the wells would diminish, and some variation of the quantum yields for isomerization with wavelength would be expected. This expectation was borne out for photoisomerization of bilirubin in NH_4OH/MeOH. The quantum yield, $\Phi_{Z,Z\rightarrow Z,E}$ for formation of the major 4*Z*,15*E* isomer declined significantly with excitation wavelength over the range of 450–500 nm. A corresponding increase in the $\Phi_{Z,Z\rightarrow E,Z}$ quantum yield was not detected for excitation from 430 to 480 nm, but the value for excitation at 500 nm was significantly greater than that for excitation at 480 nm. The possibility that the wavelength-dependent photochemistry exhibited by bilirubin in NH_4OH/MeOH stems from the presence of conformational isomers [27] or aggregates [19] or from other ground-state phenomena is ruled out by the wavelength-independent photochemistry of *BR*-III (**4**), *BR*-XIII (**5**) and *MBR*-XIII (**6**) in the same solvent.

When bilirubins bind to albumin, strong intramolecular exciton coupling is maintained, as shown by CD studies of symmetric (*BR*-III, *MBR*-XIII) and unsymmetric (*BR*-IX) rubins [15, 16, 18, 28]. Since the two chromophores of each bound pigment molecule are no longer in identical environments, the relative rates of radiationless deactivation and the partitioning of de-excitation pathways between return to the original (*Z*,*Z*) ground state and to the photoisomer ground state would be expected to be different for each of the two exciton states. Consequently, wavelength-dependent quantum yields for $Z\rightarrow E$ photoisomerization would be expected even for symmetrically substituted rubins bound to albumin. This was observed for all three of the symmetrical compounds studied, most markedly for *BR*-III (**4**). Thus, complexation with albumin desymmetrizes symmetrical rubins and induces wavelength-dependent photochemistry. Bichromophores other than rubins are likely to exhibit the same phenomenon when they bind to proteins.

In contrast to the bichromophoric rubins, the monochromophoric compound **7** (*XBR*), for which exciton coupling is impossible, showed no detectable variation in $\Phi_{Z\rightarrow E}$ over a range of wavelengths-spanning its visible absorption band in NH_4OH/MeOH or when bound to HSA.

The quantum yields for $Z\rightarrow E$ photoisomerization of the model dipyrrinone *XBR* (**7**) in NH_4OH/MeOH are considerably larger than those for $Z\rightarrow E$ photoisomerization of bilirubins in the same solvent. This is not unexpected, because intramolecular hydrogen bonding between propionic carboxylates and pyrrinone NH groups, which would raise the energy barrier for $Z\rightarrow E$ isomerization, is possible only in the rubins. Hydrogen bonding could also lower quantum yields for isomerization of the rubins by facilitating abortive radiationless relaxation processes [29, 30].

The data in this paper, along with previous work, show that quantum yields for $Z\rightarrow E$ photoisomerizations of bilirubins are remarkably sensitive to both protein binding and to the specific nature and position of the substituents on the lactam rings. Although association of the pigments with albumin might be expected intuitively to inhibit photoisomerization compared to the reaction in protein-free solvents, such as methanolic ammonia, the converse is true for *BR*-IX and *BR*-XIII. In contrast, binding to albumin has relatively little effect on photoisomerization of *MBR*-XIII, $\Phi_{Z\rightarrow E}$ values for this compound being similar in methanol and aqueous albumin solutions. However, at present, the individual influences of lactam substitution, hydrogen bonding, and protein binding on the quantum yields cannot be quantitated.

Experimental

Chemicals

Bilirubin (Porphyrin Products, Logan, UT, USA) was purified and crystallized as described previously [31]. Bilirubin IIIα (*BR*-III, **4**) and bilirubin XIIIα (*BR*-XIII, **5**) were isolated by preparative high pressure liquid chromatography (HPLC) [32] of a purified mixture of bilirubins IIIα, IXα and XIIIα produced by acid catalyzed scrambling of bilirubin [33]. Xanthobilirubic acid (*XBR*, **7**) and mesobilirubin XIIIα (*MBR*-XIII, **6**) were prepared by total synthesis [34, 35]. All pigments were >94% homogeneous by HPLC. Human serum albumin (HSA) was ''Essentially Fatty Acid Free, Fraction V'' (Sigma Chemical Co., St. Louis, MO, USA).

Solutions

Solutions in NH_4OH/MeOH were prepared by dissolving weighed amounts of solute in argon purged solvent (conc. NH_4OH:MeOH = 0.10:99.9, v/v). Solutions of rubins in aqueous HSA were prepared by dissolving weighed quantities of pigment (0.06–0.3 mg) in 50–300 µl of argon purged 0.05 *M* NaOH and diluting this solution immediately to the required concentration with HSA in argon purged 0.1 *M* phosphate buffer (*pH* 7.4). Final pigment:HSA molar concentration ratios were 1:2. For studies on *XBR* (**7**) a mole ratio of pigment to protein of 1:10 was used. With lower protein ratios, thermal reversion of *E*-**7** to *Z*-**7** was significant during the time required to complete the measurements. Solutions were freshly prepared each working day and allowed to stand for about an hour in the dark before starting measurements. Pigment solutions were manipulated under red

Table 4. Absorption maxima (λ_{max}) and millimolar extinction coefficients (ε_{max}) for pigments studied

	0.1% NH_4OH/MeOH		HSA/buffer, *pH* 7.4	
Compound	λ_{max} (nm)	ε_{max}	λ_{max} (nm)	ε_{max}
BR-IX (**1**)	453	68.4 ± 1.0	458	47.0 ± 1.3
BR-III (**4**)	455	61.1 ± 2.7	456	53.0 ± 1.0
BR-XIII (**5**)	448	57.5 ± 2.0	458	42.0 ± 1.2
MBR-XIII (**6**)	430	65.3 ± 0.5	436	50.2 ± 0.9
XBR (**7**)	416	37.5 ± 0.3	426	31.2 ± 0.4

safelight. Extinction coefficients and absorption maxima for the compounds used in the study are listed in Table 4.

Quantum yields

Solutions (1.5–2 ml) were irradiated at room temperature under 1 atmosphere of argon in a 1 cm path length quartz cuvette by a light beam with a cross section of about 0.2 cm^2 inside the solution. During irradiations, samples were stirred magnetically by a stirring bar which did not obstruct the light beam. In some experiments, irradiation was performed with 5 nm bandpass light from a Bausch and Lomb grating monochromator. The light beam was filtered to remove harmonic overtones below 360 nm. In other experiments, we used the expanded beam of an argon ion laser (Spectra Physics, Model 165–008). Energy doses in the quantum yield measurements were kept low enough to produce a fraction of *E* isomer that was less than 20% of the photoequilibrium value for each excitation wavelength. Photoequilibria for $Z \rightleftarrows E$ reactions were generated using photon fluence rates about 10 times greater than those used in the quantum yield measurements, and the reactions were monitored by absorbance difference spectroscopy. Photon dose rates at the sample surface were measured by potassium ferrioxalate actinometry [36] or by a photodiode power meter (EG & G, Model 460). The two methods gave similar results. A 0.02 *M* solution of $K_3Fe(C_2O_4)_3$ in 0.05 *M* H_2SO_4 was used as actinometer for measurements in the 390–460 nm range. The actinometer concentration was increased to 0.15 *M* for measurements between 470 and 515 nm. The light intensity was measured before and after each photoisomerization experiment, and the average value was used to calculate the incident photon dose rate. In some experiments, the excitation light was split into two orthogonal beams by a cube beam splitter in order to monitor the light intensity during the photoisomerization. Photon doses in the quantum yield measurements ranged from 4.4×10^{15} to 2.6×10^{17} depending on excitation wavelength, pigment concentration, and volume of the sample. Initial pigment concentrations were 9.3–21.9 μ*M*, 6.5–66 μ*M*, 9.9–22.6 μ*M*, 15.4–23 μ*M* and 4.2–10.5 μ*M* for *BR*-III, *BR*-IX, *BR*-XIII, *MBR*-XIII and *XBR*, respectively, in 0.1% NH_4OH/MeOH, and 23.9–51.4 μ*M*, 30.0–44.4 μ*M*, 32.7–36.8 μ*M* and 15.7–41.7 μ*M* for *BR*-III, *BR*-XIII, *MBR*-XIII and *XBR*, respectively, in aqueous HSA solutions.

Quantum yields (Φ) for the $Z \rightarrow E$ reaction were calculated by

$$\Phi = \frac{c_E \times V \times N}{F \times t \times (1 - 10^{-A})}$$

where c_E is the concentration of the *E* isomer after irradiation time *t*, *V* represents the solution volume, and *N* is *Avogadro*'s number. *F* is the photon flux and *A* the initial absorbance of the solution. The concentration of the *E* isomer in the irradiated solutions was determined by HPLC and

corrected for the $E \rightarrow Z$ back photoreaction according to

$$c_E = c_E^{PE} \times \ln\left(\frac{c_E^{PE}}{(c_E^{PE} - c_E^m)}\right)$$

where c_E^m and c_E^{PE} are the measured concentrations of the E isomer at irradiation time t and at photoequilibrium.

HPLC analyses [5, 37]

Photoisomers were analyzed on a 5μ, 25×0.46 cm Ultrasphere C18 IP-ODS column (Beckman Instruments, Inc., Fullerton, CA, USA) coupled to a 3×0.46 cm pre-column containing the same packing material. The solvent flow rate was 1 ml/min. Eluting compounds were detected with a diode array absorbance detector (Hewlett-Packard, Model 1040A). The solvent was a mixture of water and 0.1 *M* methanolic di-*n*-octylamine acetate (Me-*Docta*), prepared from di-*n*-octylamine (Aldrich Chemical Co., St. Louis, MO, USA) and acetic acid.

For analysis of the isomers of *XBR* the H_2O:Me-*Docta* ratio was 1:4 (v/v) and peaks were monitored at 416 nm, the absorption maximum for *Z-XBR* in the eluent. Preliminary studies on the $Z \rightleftarrows E$ photoisomerization of *XBR* in the HPLC mobile phase showed that the absorbance spectra of the individual isomers have an isosbestic point at 443 nm and relative extinction coefficients of 1:1.63 (*E*:*Z*) at 416 nm. This correction factor was used in calculating relative isomer concentrations from the integrated areas of HPLC peaks detected at 416 nm.

For HPLC analysis of *BR*-III and *BR*-IX isomer solutions, the H_2O:Me-*Docta* ratio was 8:92 (v/v); for analysis of *MBR*-XIII solutions it was 5:95 (v/v), and for analysis of *BR*-XIII solutions it was either 8:92 (v/v) (photolyses in NH_4OH/MeOH) or 5:95 (v/v) (photolyses in HSA solutions). For *BR*-III, *BR*-XIII and *MBR*-XIII, peaks were monitored at the corresponding isosbestic points (481, 486, and 455 nm, respectively) for the $Z \rightleftarrows E$ isomerization in the HPLC solvent, determined by absorbance difference spectroscopy. Photoisomers of *BR*-IX were monitored at 450 nm, and relative HPLC peak areas were corrected for extinction coefficient differences using the factors of 1.00, 1.02 and 1.25 for 4*Z*,15*Z*-, 4*E*,15*Z*- and 4*Z*,15*E*-*BR*-IX, respectively [12].

Injection volumes for HPLC were 20 μl. Samples in NH_4OH/MeOH were mixed before injection with enough water to make the proportion of water in injectate and mobile phase the same. This precaution eliminated ghost peaks that interfered with the quantitation of *E* isomers. Samples in HSA solutions were diluted with excess ice-cold mobile phase, vortexed for a few seconds, microfuged for 1 min, and the clear fluid phase was injected. Dilution ranged from 1:8 for *BR*-III/HSA solutions to 1:2 for *XBR*/HSA solutions.

In photoisomerization experiments, samples were analyzed in duplicate or triplicate either immediately or after brief storage at 0 °C. Unirradiated solutions were analyzed as controls. Several experiments (3–5) were run for each excitation wavelength, and average values were calculated. *E* photoisomers were identified on the basis of their absorption spectra, HPLC retention times, and their quantitative reversion to the corresponding *Z* isomers upon treatment with trifluoroacetic acid [5]. The significance of the wavelength dependence was tested by one-way analysis of variance. Curves in the displayed figures were drawn using the linear fit command in Kaleidograph (Macintosh Version 3.0, Abelbeck Software, Reading, PA, USA).

Acknowledgements

This work was supported by grants DK 26307, DK 26743, GM 36633, and HD 17779 from the National Institutes of Health and by NATO grant 0149/85. *G. A.* was supported by a fellowship from the *Comitato Nazionale per le Scienze Biologiche e Mediche* – CNR, Italy. Also acknowledged are the assistance of Dr. *Franco Fusi* (CNR) with some of the measurements and support and encouragement to *G. A.* by Prof. *R. Pratesi* (CNR).

References

[1] Morrison H, Bernasconi C, Pandey G (1984) Photochem Photobiol **40**: 549
[2] Agati G, Fusi F, Pratesi R, McDonagh AF (1992) Photochem Photobiol **55**: 185
[3] Lightner DA, McDonagh AF (1984) Acc Chem Res **17**: 417
[4] McDonagh AF (1986) N Engl J Med **314**: 121
[5] McDonagh AF, Palma LA, Trull FR, Lightner DA (1982) J Am Chem Soc **104**: 6865
[6] Kanna Y, Arai T, Tokumaru K (1993) Bull Chem Soc Jpn **66**: 1586
[7] McDonagh AF, Lightner DA (1985) Pediatrics **75**: 443
[8] Ennever JF (1992) Phototherapy for Neonatal Jaundice. In: Polin R, Fox W (eds) Fetal and Neonatal Physiology, vol 2. Saunders, New York, p 1165
[9] Harada N, Nakanishi K (1983) Circular Dichroic Spectroscopy – Exciton Coupling in Organic Stereochemistry. University Science Books, Mill Valley, CA
[10] McDonagh AF, Lightner DA (1985) Mechanism of Phototherapy of Neonatal Jaundice. Regiospecific Photoisomerization of Bilirubins. In: Blauer G, Sund H (eds) Optical Properties and Structure of Tetrapyrroles. Walter de Gruyter, Berlin, p 297
[11] McDonagh AF, Lightner DA (1985) Intramolecular Energy Transfer in Bilirubins. In: Bensasson R, Jori G, Land E, Truscott T (eds) Primary Photoprocesses in Biology and Medicine. Plenum Press, New York, p 321
[12] McDonagh AF, Agati G, Fusi F, Pratesi R (1989) Photochem Photobiol **50**: 305
[13] Lamola AA, Braslavsky SE, Schaffner K, Lightner DA (1983) Photochem Photobiol **37**: 263
[14] Kanna Y, Arai T, Tokumaru K (1993) Bull Chem Soc Jpn **66**: 1482
[15] Blauer G (1983) Israel J Chem **23**: 201
[16] Person RV, Peterson BR, Lightner DA (1994) J Am Chem Soc **116**: 42
[17] Boiadjiev SE, Lightner DA (1997) Chirality **9**: 604
[18] Lightner DA, Reisinger M, Landen GL (1986) J Biol Chem **261**: 6034
[19] Kasha M (1963) Radiation Res **20**: 55
[20] Falk H, Neufingerl F (1979) Monatsh Chem **110**: 987
[21] Falk H, Neufingerl F (1979) Monatsh Chem **110**: 1243
[22] Falk H, Grubmayr K, Neufingerl F (1979) Monatsh Chem **110**: 1127
[23] Kaschke M, Kleinschmidt J, Riegler M (1986) Chem Phys **107**: 89
[24] Lamola AA (1985) Effects of Environment on Photophysical Processes of Bilirubin. In: Blauer G, Sund H (eds) Optical Properties and Structure of Tetrapyrroles. Walter de Gruyter, Berlin, p 311
[25] Ikeda T, Lee B, Kurihara S, Tazuke S, Takenaka A, Ito S, Yamamoto M (1988) J Am Chem Soc **110**: 8299
[26] Ikeda T, Lee B, Tazuke S, Takenaka A (1990) J Am Chem Soc **112**: 4650
[27] Holzwarth AR, Schaffner K (1981) Photochem Photobiol **33**: 635
[28] Agati G, McDonagh AF (1995) J Am Chem Soc **117**: 4425
[29] Falk H (1989) The Chemistry of Linear Oligopyrroles and Bile Pigments. Springer, Wien
[30] Lewis FD, Yoon BA, Arai T, Iwasaki T, Tokumaru K (1995) J Am Chem Soc **117**: 3029
[31] McDonagh AF, Assisi F (1972) Biochem J **129**: 797
[32] DiCesare JL, Vandemark FL (1987) Perkin Elmer Chromatog Newslet **9**: 7
[33] McDonagh AF, Assisi F (1972) J Chem Soc Chem Comm 117
[34] Grunewald J, Cullen R, Bredfeldt J, Strope ER (1975) Org Prep Proc Int **7**: 103
[35] Trull FR, W FR, Lightner DA (1987) J Heterocyclic Chem **24**: 1573
[36] Murov SL (1973) Handbook of Photochemistry. Dekker, New York
[37] McDonagh AF, Palma LA, Lightner DA (1982) J Am Chem Soc **104**: 6867

Received January 13, 1998. Accepted January 27, 1998